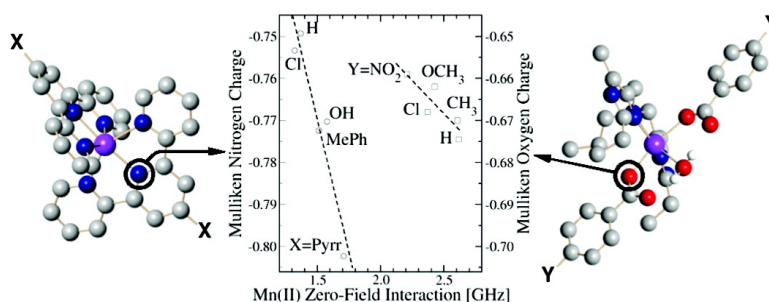


## The Relationship between the Manganese(II) Zero-Field Interaction and Mn(II)/Mn(III) Redox Potential of Mn(4'-X-terpy) Complexes

Jessica Gtjens, Martin Sjdin, Vincent L. Pecoraro, and Sun Un

*J. Am. Chem. Soc.*, **2007**, 129 (45), 13825-13827 • DOI: 10.1021/ja076024o • Publication Date (Web): 25 October 2007

Downloaded from <http://pubs.acs.org> on February 14, 2009



### More About This Article

Additional resources and features associated with this article are available within the HTML version:

- Supporting Information
- Links to the 4 articles that cite this article, as of the time of this article download
- Access to high resolution figures
- Links to articles and content related to this article
- Copyright permission to reproduce figures and/or text from this article

[View the Full Text HTML](#)



## The Relationship between the Manganese(II) Zero-Field Interaction and Mn(II)/Mn(III) Redox Potential of Mn(4'-X-terpy)<sub>2</sub> Complexes

Jessica Gätjens,<sup>‡</sup> Martin Sjödin,<sup>†</sup> Vincent L. Pecoraro,<sup>‡</sup> and Sun Un\*<sup>†</sup>

Service de Bioénergétique Biologie Structurale et Mécanismes, CNRS URA 2096, Institut de Biologie et Technologies de Saclay, CEA Saclay, 91191 Gif-sur-Yvette, France, and Department of Chemistry, University of Michigan, Ann Arbor, Michigan 48109-1055

Received August 10, 2007; E-mail: sun.un@cea.fr

Divalent manganese, Mn(II), plays an important role in a variety of biological processes.<sup>1,2</sup> Although crystallographic structures have been useful in understanding the overall physical structures of manganese binding sites in proteins, they are often insufficient for understanding the electronic and chemical properties of these ions in proteins. Electron paramagnetic resonance (EPR) spectroscopy is one of the few techniques that can selectively detect and be used to characterize Mn(II) ions. A Mn(II) EPR spectrum is defined by the spin Hamiltonian

$$H = g\beta BS_z + A I_z S_z + \frac{D}{3}(3S_z^2 - S(S+1)) + \frac{E}{2}(S_+^2 + S_-^2)$$

where the first term is the Zeeman interaction, the second the electron–nuclear hyperfine interaction, and the last two terms describe the zero-field interaction. For most Mn(II) ions, the Zeeman and hyperfine interactions are isotropic.<sup>3</sup> The size of the hyperfine coupling has been related to ligand–metal covalency,<sup>4</sup> but the variation in their values is relatively small (<50 MHz) compared to the zero-field interaction, which, by contrast, is anisotropic and ranges from 0 to values greater than 10 GHz.

The zero-field interaction in powder or frozen solutions can be determined using high-frequency high-field EPR (HFEP). In this case, a large magnetic field is applied so that energies of the six electronic spin states are dominated by the Zeeman interaction and essentially become  $m_s g\beta B$  where  $m_s = \{-5/2, -3/2, -1/2, 1/2, 3/2, \text{ and } 5/2\}$ . When sufficiently low temperatures are used ( $T < hv/k$  or 11 K at 285 GHz 10 T experiments), only the  $m_s = -5/2$  level is thermally populated and the HFEP spectrum is essentially of that transition (Figure S1). The zero-field parameters can be directly obtained from the “turning points” of such spectra (Figure 1).

The relationship of the zero-field parameters  $D$  and  $E$  to the chemical and physical properties of Mn(II) is poorly understood. There are diverse views on the influence of coordination number, ligand atom types, and symmetry on the Mn(II) zero-field interaction.<sup>5–7</sup> It would be interesting and useful for understanding enzymatic chemistry to establish whether there is a direct correlation between the zero-field parameters and the metal redox properties since measurements of  $D$  and  $E$  values are often more straightforward, especially for enzyme intermediates, than determination of redox potentials. To this end, we have examined the zero-field parameters and redox potentials of a series of closely related complexes, Mn(II)(4'-X-terpy)<sub>2</sub>, where X's are substituents that have varied electron-donating/withdrawing capacities (Scheme 1 and Figure S2).<sup>8–10</sup> The high-field EPR 4.2 K spectra of these complexes in acetonitrile solution are shown in Figure 1. The greater than

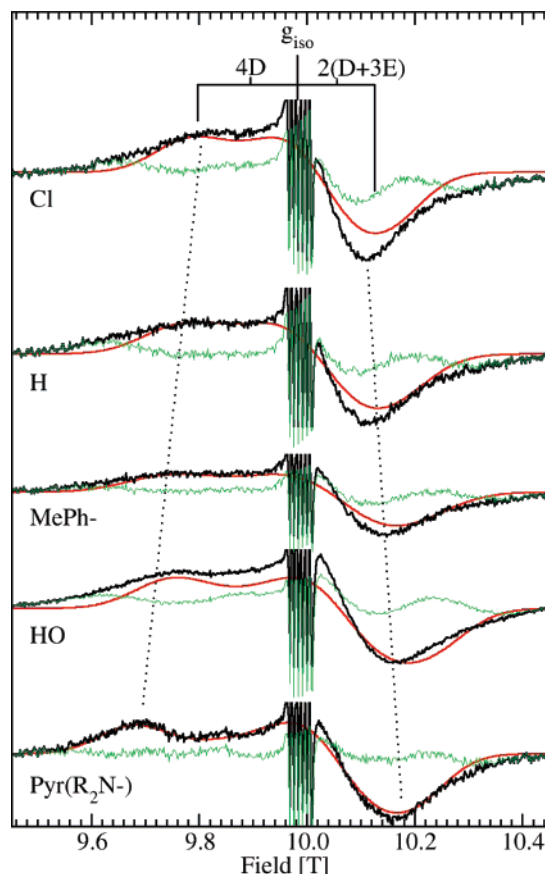
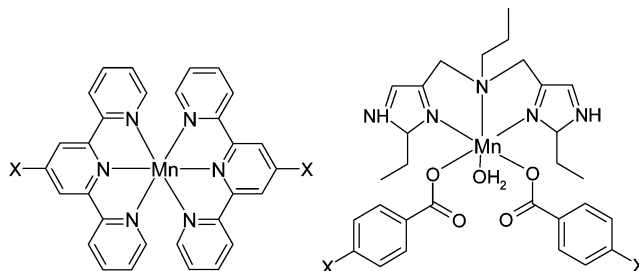


**Figure 1.** The 4.2 K 279 GHz HFEP spectra of the 2 mM acetonitrile solutions of Mn(4'-X-terpy)<sub>2</sub> complexes containing 100 mM tetrabutylammonium hexafluorophosphate: the experimental spectrum (black), simulation (red), and residual (green). In some cases, the sharp six lines in the center of the spectrum arise from the  $m_s = -1/2 \rightarrow 1/2$  transitions and have been artificially truncated. The labels at the left correspond to the X substituent in Scheme 1.

**Scheme 1.** MnTerpy (left) and MnBIAP (right) Complexes



expected intensity of the six sharp lines arising from the  $m_s = -1/2 \rightarrow 1/2$  transitions indicated that small amounts of complexes

<sup>†</sup> Institut de Biologie et Technologies de Saclay.

<sup>‡</sup> University of Michigan.

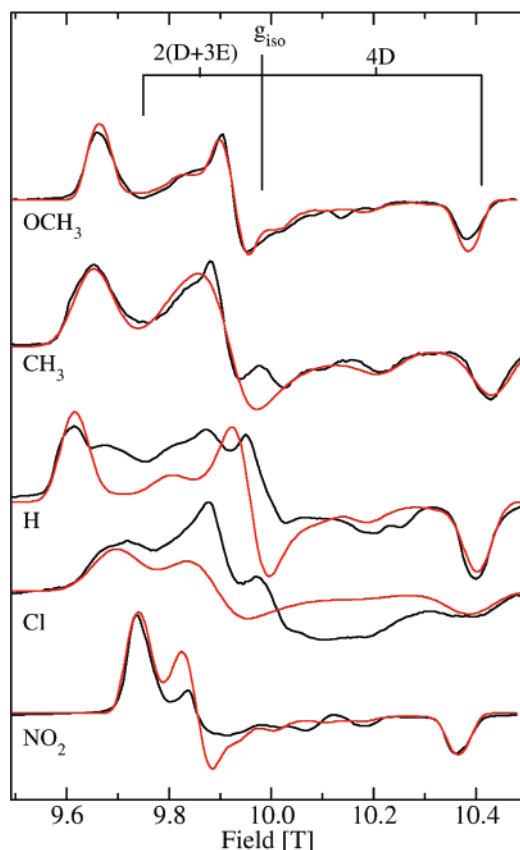


**Figure 2.** The 4.2 K 279 GHz HFEPR spectrum of powder MnBIAP samples (black) and simulations (red). The labels at the left correspond to the X substituent in Scheme 1.

decomposed in solution. The spectra were fitted based on the above spin Hamiltonian in order to obtain the zero-field parameters. For all of the complexes, the zero-field  $D$  parameters were found to be negative. The simulations also indicated the presence of a minority species for which the zero-field interaction was slightly larger. The same solutions used to record the HFEPR spectra were also used for redox potential measurements.<sup>11</sup>

There was good reason to believe that the Mn(II)/Mn(III) redox potential and Mn(II) zero-field interaction might be correlated. It has been shown that the zero-field interaction is sensitive to local electrostatic interactions that presumably would also affect the redox potentials.<sup>12</sup> The data shown in Figure 3 demonstrate that the relationship is close to linear for  $D$  but nearly invariant with respect to  $E$ . Density functional calculations were performed to obtain relevant charge densities: first the optimized structures were obtained using Gaussian03<sup>13</sup> and the B3LYP/LANL2DZ hybrid density functional and basis-set combination and the Mulliken charges from subsequent B3LYP/6-311G calculations.<sup>14–21</sup> The Mulliken charges of the central terpy nitrogens were found to be linearly related to the zero-field interaction (Figure 4). This correlation implied that the electrochemistry of the Mn(II) was also associated with the charge on these nitrogen atoms.

We tested the generality of these relationships by examining a second set of Mn(II) complexes formed with *N,N*-bis(2-ethyl-5-methylimidazol-4-ylmethyl)aminopropane (BIAP).<sup>22–24</sup> This ligand provided three nitrogen donor atoms, one from a tertiary amine and two from imidazole moieties. In addition, three oxygen atoms from a water molecule and two benzoic acids that were *para*-substituted with OCH<sub>3</sub>, CH<sub>3</sub>, H, Cl, and NO<sub>2</sub> (Scheme 1) completed the metal coordination sphere. The powder HFEPR spectra of these complexes are shown in Figure 2. The spectrum of the H-substituted

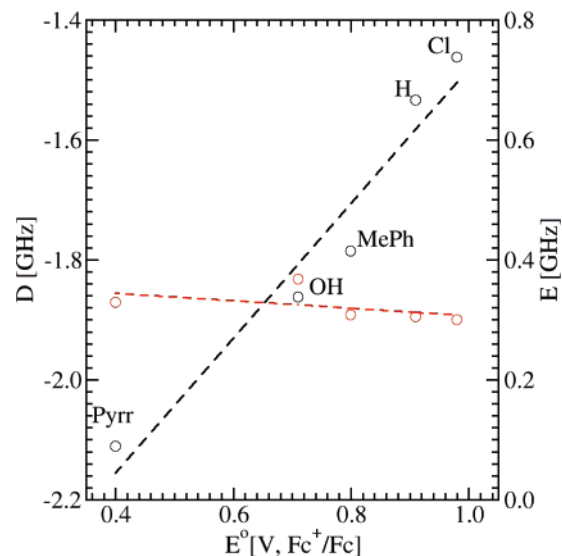


**Figure 3.** Correlation between the Mn(II) zero-field  $D$  (black) and  $E$  (red) parameters and the Mn(II)/Mn(III) redox potentials of Mn(terpy) complexes. The dashed lines are linear regression fits.

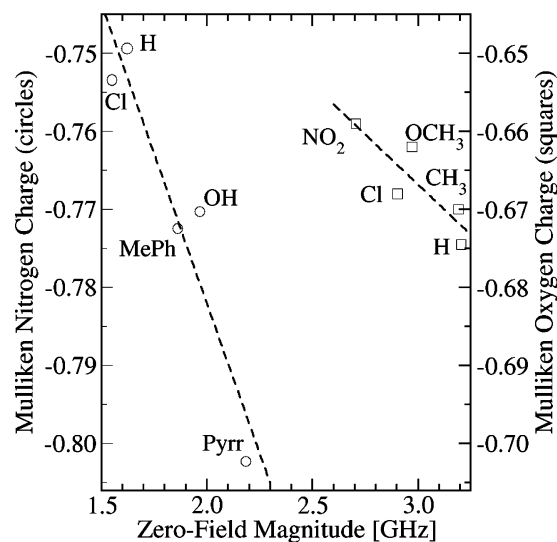


**Figure 4.** Relationship between magnitudes of the Mn(II) zero-field interaction and the B3LYP/6-311G Mulliken 4'-nitrogen charges of the Mn(terpy) complexes (left scale and circles) and the carboxylate oxygen charges of the MnBIAP complexes (right scale, squares). The dashed lines are linear regression fits.

complex appeared to be composed of two overlapping components, while the Cl-substituted derivative appeared to have significant contributions from a contaminating species with markedly smaller zero-field interaction (Figure 2). In contrast, the frozen acetonitrile solution spectra in all but the Cl-substituted complex were much narrower and essentially featureless (Figure S4). This indicated that the BIAP zero-field interactions in frozen solutions were significantly smaller but, at the same time, more distributed than in crystals. Redox measurements also yielded nonideal data. This strongly suggested that dissolution of the BIAP complexes was accompanied by considerable changes and disorder in the ligand sphere, rendering comparisons between solution zero-field interaction and redox potential of these complexes far less meaningful than for the terpy complexes. Nonetheless, for all of the BIAP complexes, it was possible to obtain accurate estimates of the zero-field interaction in the solid state by fitting the extreme edges of the powder spectra. In contrast to the Mn(terpy) complexes in

solution, all of the BIAP complexes had positive  $D$  values and their  $E$  parameters varied significantly with the substituent. The sign of  $D$  was also readily apparent from the observation that all the BIAP spectra extended further to the high-field side of the magnetic field position corresponding to  $g_{\text{iso}}$  than to the low-field side. The magnitude of the BIAP zero-field interaction, as measured by the quantity  $(D^2 + 3E^2)^{1/2}$  correlated linearly with the charge of the ligating atom most affected by the substitution, the carboxyl oxygen atom (Figure 4). Likewise, the frozen solution Mnterpy zero-field interaction depended linearly on the center nitrogen charge. Since the same linear response was seen for two very different ligand spheres, we conclude that it is likely to be a general property of Mn(II) complexes. As the relationship between electron-donating capacity of a substituent and redox potential also appears to be general,<sup>25–27</sup> it is likely that the variation in the redox potentials of related Mn(II) complexes will be mirrored in their zero-field interactions in a linear manner as is the case for the Mnterpy complexes.

These conclusions are especially noteworthy since a number of Mn(II) protein centers with histidine and carboxylic acid ligands have very similar ligand spheres to that of the BIAP complexes. For example, the significant differences of 0.5 and 0.1 GHz in  $E$  and  $D$  values, respectively, between manganese and manganese reconstituted iron superoxide dismutases from *E. coli*<sup>28</sup> may reflect the large difference of  $>0.7$  V in redox potentials determined by Miller.<sup>29</sup>

Mn(II) zero-field interactions will be a new way of looking at manganese binding proteins. This approach can semiquantitatively estimate differences in potentials of intermediates that can be trapped and examined by HFEPFR and that may not be sufficiently stable for direct measurements using traditional redox techniques.

**Acknowledgment.** Financial support was provided by the Swedish Research Council (M.S.) and the Sixth Framework Program of the European Union through the Solar H NEST STRP network (M.S.) and a Feodor Lynen fellowship from the Alexander von Humboldt Foundation (J.G.). We thank L. Tabares for invaluable discussions, and C. Hureau for assistance.

**Supporting Information Available:** Energy levels diagrams, solution HFEPFR BIAP complex spectra, line drawings of molecules studied and comparisons of the powder and frozen solution spectra, complete citation for reference 13, and derivation of the expression for the magnitude of the zero-field interaction. This material is available free of charge via the Internet at <http://pubs.acs.org>.

## References

- Yocum, C. F.; Pecoraro, V. L. *Curr. Opin. Chem. Biol.* **1999**, *3*, 182–187.
- Papp-Wallace, K. M.; Maguire, M. E. *Annu. Rev. Microbiol.* **2006**, *60*, 187–209.
- Griffith, J. S. *The Theory of Transition-Metal Ions*; Cambridge University Press: Cambridge, 1961.
- van Wieringen, J. S. *Discuss. Faraday Soc.* **1955**, *19*, 118–126.
- Tabares, L. C.; Cortez, N.; Agalidis, I.; Un, S. *J. Am. Chem. Soc.* **2005**, *127*, 6039–6047.
- Walsby, C. J.; Telsler, J.; Rigsby, R. E.; Armstrong, R. N.; Hoffman, B. M. *J. Am. Chem. Soc.* **2005**, *127*, 8310–8319.
- Carnieli, R.; Larsen, T. M.; Reed, G. H.; Zein, S.; Neese, F.; Goldfarb, D. *J. Am. Chem. Soc.* **2007**, *129*, 4240–4252.
- Rao, J. M.; Hughes, M. C.; Macero, D. J. *Inorg. Chim. Acta* **1976**, *18*, 127–131.
- Morrison, M. M.; Sawyer, D. T. *Inorg. Chem.* **1978**, *17*, 333–337.
- Following procedures described in the literature,<sup>8,9</sup> we isolated the  $[\text{Mn}(4\text{-X-terpy})_2](\text{ClO}_4)_2$  complexes from the reaction of  $\text{Mn}(\text{ClO}_4)_2 \cdot 6\text{H}_2\text{O}$  and the respective ligand. In general, a solution (slurry) of the appropriate ligand (0.6 mmol) in 12 mL of hot ethanol was added to a solution of  $\text{Mn}(\text{ClO}_4)_2 \cdot 6\text{H}_2\text{O}$  (0.25 mmol) in 5 mL of distilled water. In most cases, the immediate formation of a precipitate was observed. The yellow mixture was stirred for 2 h and then filtered. The yellow precipitate was washed with small amounts of ethanol and diethyl ether. In order to increase the yields, the filtrate solution was further concentrated.
- Electrochemical measurements were carried out at ambient temperature in a 0.1 M tetrabutylammonium hexafluorophosphate (TBAPF<sub>6</sub>) (Fluka electrochemical grade)/acetonitrile (Sigma Aldrich, HPLC grade) solution with an analyte concentration of 2 mM. The solvent was dried over 8–12 mesh molecular sieves (Aldrich), and the analyte solution was purged with argon and kept under argon atmosphere during measurement. A conventional three-electrode system connected to a CH Instruments electrochemical workstation (CHI660C) was used. The reference electrode (Ag/AgCl in saturated KCl<sub>aq</sub>) that was kept in a separate compartment filled with electrolyte solution and connected to the analyte solution by a glass frit was calibrated versus ferrocene using the same conditions as for the sample after each measurement series. A commercial glassy carbon electrode with a diameter of 3 mm was used as working electrode, and a freshly annealed platinum wire served as auxiliary electrode. The glassy carbon working electrode was polished on 0.3 alumina (Buehler) before each series of measurement or, when required due to adsorption of the analyte, after each measurement. Cyclic voltammograms (CV) were typically recorded at a scan rate of 0.1 V/s, and the reported data are from reproducible voltammograms from multiple consecutive scans centered on the recorded redox process.
- Tabares, L. C.; Cortez, N.; Hiraoka, B. Y.; Yamakura, F.; Un, S. *Biochemistry* **2006**, *45*, 1919–1929.
- Frisch, M. J.; et al. *Gaussian 03*, revision B.05; Gaussian Inc.: Wallingford, CT, 2003.
- Becke, A. D. *J. Chem. Phys.* **1993**, *98*, 5648–5652.
- Hay, P. J. *J. Chem. Phys.* **1977**, *66*, 4377–4384.
- Hay, P. J.; Wadt, W. R. *J. Chem. Phys.* **1985**, *82*, 270–283.
- Hay, P. J.; Wadt, W. R. *J. Chem. Phys.* **1985**, *82*, 299–310.
- Krishnan, R.; Binkley, J. S.; Seeger, R.; Pople, J. A. *J. Chem. Phys.* **1980**, *72*, 650–654.
- Lee, C. T.; Yang, W. T.; Parr, R. G. *Phys. Rev. B* **1988**, *37*, 785–789.
- Vosko, S. H.; Wilk, L.; Nusair, M. *Can. Phys. J.* **1980**, *58*, 1200–1211.
- Wadt, W. R.; Hay, P. J. *J. Chem. Phys.* **1985**, *82*, 284–298.
- Bouwman, E.; Douziche, B.; Gutierrez-Soto, L.; Beretta, M.; Driessen, W. L.; Reedijk, J.; Mendoza-Diaz, G. *Inorg. Chim. Acta* **2000**, *304*, 250–259.
- Warzeska, S. T.; Micciche, F.; Mimmi, M. C.; Bouwman, E.; Kooijman, H.; Spek, A. L.; Reedijk, J. *J. Chem. Soc., Dalton Trans.* **2001**, 3507–3512.
- Following a modified procedure of Reedijk and co-workers,<sup>22,23</sup> for the synthesis of the BIAP complexes, we added a solution of the BIAP ligand (0.5 mmol) in 1 mL of methanol to a solution of  $\text{Mn}(\text{ClO}_4)_2 \cdot 6\text{H}_2\text{O}$  (0.5 mmol) in 1 mL of methanol. After 10 min of stirring under nitrogen, a solution of the corresponding benzoic acid derivative (1.0 mmol in 1 mL of H<sub>2</sub>O, X = H, sodium salt; 1.0 mmol in 1 mL of CH<sub>3</sub>CN, addition of 10 drops of triethylamine, X = Cl, OCH<sub>3</sub>, CH<sub>3</sub>NO<sub>2</sub>) was added. In most cases, the formation of a white precipitate was observed. Usually, about 10 mL of H<sub>2</sub>O was added in order to increase the yield. The precipitate was filtered off and washed with small amounts of water and dried.
- Lewis, E. A.; Smith, J. R. L.; Walton, P. H.; Archibald, S. J.; Foxon, S. P.; Giblin, G. M. *J. Chem. Soc., Dalton Trans.* **2001**, 1159–1161.
- Palopoli, C.; Gonzalez-Sierra, M.; Robles, G.; Dahan, F.; Tuchagues, J. P.; Signorella, S. *J. Chem. Soc., Dalton Trans.* **2002**, 3813–3819.
- Chambers, J.; Eaves, B.; Parker, D.; Claxton, R.; Ray, P. S.; Slattery, S. *J. Inorg. Chim. Acta* **2006**, *359*, 2400–2406.
- Un, S.; Tabares, L. C.; Cortez, N.; Hiraoka, B. Y.; Yamakura, F. *J. Am. Chem. Soc.* **2004**, *126*, 2720–2726.
- Miller, A.-F. In *Handbook of Metalloproteins*; Messerschmidt, A., Huber, R., Wieghardt, K., Paulos, T., Eds.; Wiley and Sons: Chichester, UK, 2001; Vol. 1, pp 668–682.

JA076024O